Monthly Notices of the ROYAL ASTRONOMICAL SOCIETY
MNRAS Advance Access published January 27, 2014
MNRAS (2014) doi:10.1093/mnras/stt2365

Decoupled gas kinematics in isolated S0 galaxies

Ivan Yu. Katkov,[1,2]★ Olga K. Sil'chenko[1,3] and Victor L. Afanasiev[4]

[1] *Sternberg Astronomical Institute, Lomonosov Moscow State University, Universitetski prospect 13, 119992 Moscow, Russia*
[2] *Faculty of Physics, Lomonosov Moscow State University, Leninskie gory 1, 119991 Moscow, Russia*
[3] *Isaac Newton Institute of Chile, Moscow Branch, Universitetski prospect 13, 119991 Moscow, Russia*
[4] *Special Astrophysical Observatory, 369167 Nizhnij Arkhyz, Russia*

Accepted 2013 December 5. Received 2013 December 5; in original form 2013 August 6

ABSTRACT

A sample of completely isolated S0 galaxies has been studied by means of long-slit spectroscopy at the Russian 6-m telescope. Seven of 12 galaxies have revealed the presence of extended ionized-gas discs whose rotation is mostly decoupled from the stellar kinematics. Five of these seven (71 ± 17 per cent) galaxies show a visible counterrotation of the ionized-gas component with respect to the stellar component. The emission-line diagnostics demonstrates a wide range of gas excitation mechanisms, although pure excitation by young stars is rare. We conclude that in all cases the extended gaseous discs in our sample S0s are of external origin, despite the visible isolation of the galaxies. Possible sources of external accretion, such as systems of dwarf gas-rich satellites or cosmological cold-gas filaments, are discussed.

Key words: galaxies: elliptical and lenticular, cD – galaxies: evolution – galaxies: ISM – galaxies: kinematics and dynamics.

1 INTRODUCTION

One of the central topics in current extragalactic astronomy is how galaxies form and how their properties change through cosmic times. This is a particularly difficult task with regards to lenticular galaxies because this class of objects shows a diversity in properties that goes beyond present-day simulations. Many internal and external physical processes controlling the evolution of galaxies through cosmic time may, and must, play a role. External processes – gravitational tides, major and minor mergers (both dry and wet), external cold gas accretion through the intergalactic medium, ram pressure in the hot intracluster/intragroup medium – govern star formation (SF) and reshape general structures. Internal disc instabilities can provoke secular evolution and matter radial redistribution. The main point is to study galaxies where manifold processes are constrained and so evolution is only driven by a few main processes. Isolated galaxies are such galaxies.

We have compiled our sample of isolated S0 galaxies based on the approaches recently developed by the team of Karachentsev, Makarov, and co-authors. Their group-finding algorithm, which takes into account the individual characteristics of galaxies, has already been used to study the properties of isolated galaxies (Karachentsev et al. 2011), binary (Karachentsev & Makarov 2008) and triple (Makarov & Karachentsev 2009) systems of galaxies and galaxy groups (Makarov & Karachentsev 2011). Our sample objects, 18 S0 galaxies that are rather nearby, $V_r < 3500$ km s^{-1}, and relatively luminous, $M_K < -19$, satisfy the following criterion of isolation: isolation index $\kappa > 2.5$. We have undertaken long-slit spectroscopy of 12 targets at the Russian 6-m telescope; seven of these have revealed extended emission lines, and among those, five galaxies demonstrate decoupled gas kinematics with respect to their stellar components. In the remaining five galaxies, the emission lines are undetectable. Previously, Davis et al. (2011) studied three galaxies of our list using their integral field unit (IFU) data; they mentioned the kinematical misalignment of stars and ionized gas in these galaxies.

Although lenticular galaxies typically have smaller amounts of cold gas than spiral galaxies, it is now becoming clear that atomic and/or molecular gas is present perhaps in most of them (Welch & Sage 2003; Sage & Welch 2006; Welch, Sage & Young 2010; Young et al. 2011), though less than half of S0 galaxies with extended cold-gas discs experience current SF (Pogge & Eskridge 1993). The frequent incidence of decoupled gas kinematics in S0s allowed Bertola, Buson & Zeilinger (1992) to conclude that at least 40 per cent of emission-line S0s acquired their gas from external sources. Based on a larger S0 sample, Zeilinger, Bertola & Buson (1993) found that half of all nearby S0s with extended ionized-gas emission possess decoupled gas kinematics. However, environment may be important here. In a recent study, Davis et al. (2011) have shown that among the Virgo cluster S0s the gaseous and stellar components always demonstrate kinematical alignment while the non-Virgo S0s, those in groups and in fields, have decoupled gas kinematics in 50 per cent of all cases. Our sample – the strictly isolated S0s – represents the extreme case of sparse environment, so if the role of environment is such as Davis et al. (2011) indicate, we could expect a large fraction of decoupled gas kinematics just within our sample.

This paper is organized in the following way. In Section 2 we describe our observations and data analysis approaches. In Section 3,

★ E-mail: katkov.ivan@gmail.com

we present our results on the gas and star kinematics in the S0 galaxies where we have detected emission lines, and in Section 4 we discuss and conclude.

2 OBSERVATIONS AND DATA REDUCTION

Spectral observations of our sample of lenticular galaxies were carried out with the multimode focal reducer SCORPIO-2 (Afanasiev & Moiseev 2011) at the 6-m telescope of the Special Astrophysical Observatory of the Russian Academy of Sciences. Long-slit spectra of all galaxies besides NGC 6654 were acquired using the VPHG1200@540 grating, which provided an intermediate spectral resolution FWHM $\approx$ 4 Å in a wavelength region from 3800 to 7300 Å. The spectrum of NGC 6654 was collected using the other grating, VPHG2300, which provided a slightly higher spectral resolution FWHM $\approx$ 2.2 Å in a shorter wavelength region from 4800 to 5600 Å. All observations were taken with a slit that was 1 arcsec wide, aligned along the major axes of the galaxies. Observations of the galaxies with the VPHG1200@540 grating were exposed using the CCD 2 k $\times$ 4 k chip E2V CCD42-90 while spectra obtained with the VPHG2300 were collected with the EEV 42-40 2 k $\times$ 2 k CCD. In both cases, a scale along the slit was 0.357 arcsec pixel^{-1}. General characteristics of the galaxies, as well as observation dates, total exposure times and atmospheric seeing conditions, are listed in Table 1.

The primary data reduction comprised the following steps: bias subtraction, flat-fielding, removing cosmic ray hits using the Laplacian filtering technique (van Dokkum 2001) and building the wavelength solution using the He–Ne–Ar arc-line spectra with accuracies of 0.1 and 0.05 Å for two grating set-ups. To subtract the sky background, we have recently invented a rather sophisticated approach (Katkov & Chilingarian 2011). We constructed a model of the spectral instrumental response of the spectrograph (line spread function – LSF) varied along and across the wavelength direction by using the twilight spectrum. The final stages of the long-slit spectra reduction were night-sky spectrum subtraction taking into account the LSF variations, spectra linearization and, to take into account spectral sensitivity variations, flux calibration by using the spectrum of a spectrophotometric standard star. The uncertainty frames were initially computed from the photon statistics and the read-out noise values, and then processed using exactly the same data reduction steps in order to estimate the flux accuracy.

2.1 Stellar kinematics

To derive information about stellar and ionized gas kinematics we first fitted the stellar absorption spectra using the PEGASE.HR high-resolution stellar population models (Le Borgne et al. 2004) convolved with a parametric line-of-sight (LOS) velocity distribution by applying the NBURSTS full spectral fitting technique (Chilingarian et al. 2007a,b). Before the minimization procedure, the model grid of stellar population spectra is convolved with the LSF. Multiplicative Legendre polynomials are also included to take into account possible internal dust reddening and residual spectrum slope variations due to the errors in the assumed instrument spectral response. Ionized-gas emission lines and remnants of the subtracted strong airglow lines do not affect the solution because of the masking of the narrow 15 Å-wide regions around them. The resulting stellar parameters are LOS velocity v, velocity dispersion σ, higher-order Gauss–Hermite moments h_3, h_4, and the stellar population parameters: the age T and metallicity [Z/H]. In this paper, we discuss only kinematics, while the stellar population properties will be considered in a forthcoming publication. LOS velocities and velocity dispersions for the stars derived along the major axes are shown in Fig. 1.

2.2 Ionized gas

The forthcoming analysis concerns the optical emission lines of the ionized gas. We subtracted the best-fitting stellar model from the observed spectrum and fitted the remaining pure emission lines by Gaussians pre-convolved with the spectrograph LSF. In such a way, we have measured LOS gas velocities and emission-line fluxes varying along the slit. Radial profiles of gaseous kinematics are also

Table 1. Global parameters of the isolated S0 galaxies with emission lines.

Galaxy	NGC 2350	NGC 3248	NGC 6654	NGC 6798	NGC 7351	UGC 4551	UGC 9519
Type (NED[a])	S0/a	S0	(R')SB0/a(s)	S0	SAB0^0?	S0?	S0?
R_{25}, kpc (NED+RC3[b])	5.6	9.2	11.3	7.1	1.9	7.8	2.9
R_{25}, arcsec (NED+RC3)	40.5	75.35	78.9	47.5	53.35	61.25	23.8
B_T^0 (LEDA[c])	13.19	13.80	12.52	13.72	13.39	13.27	14.22
M_K (NED+LEDA)[d]	–22.73	–21.82	–23.83	–23.52	–20.92	–22.63	–21.71
V_r, km s^{-1} (NED)	1910	1523	1821	2390	890	1749	1692
Distance, Mpc (NED)	28.7	25.3	29.5	30.8	7.3	26.2	25.4
Inclination, deg (LEDA)	68.4	70.6	44.7	90.0	76.4	90.0	23.2
PA_{phot}, deg (LEDA)	110	135	7.5	146	1.7	111.5	–
$\sigma_\star$, km s^{-1} (LEDA)	–	–	158	162	50	167	112
$M_{\mathrm{H\,I}}$, 10^9 M$_\odot$ [e]	–	<0.017	–	2.4	–	<0.018	1.86
$M_{\mathrm{H_2}}$, 10^8 M$_\odot$ [f]	–	<0.36	–	0.68	–	<0.42	5.89
Obs. date	2012 Dec 12	2012 Apr 22	2012 Sep 20	2011 Nov 20	2011 Nov 19	2012 Dec 12	2012 Apr 21
Exp. time, s	6000	2700	6600	5400	3600	8400	4500
Seeing, arcsec	1.6	3.0	1.3	2.5	2.0	2.0	2.0

[a]NASA/IPAC Extragalactic Database.
[b]Third Reference Catalogue of Bright Galaxies.
[c]Lyon-Meudon Extragalactic Database.
[d]Makarov et al. data base based on LEDA and NED.
[e]Serra et al. (2012).
[f]Young et al. (2011).

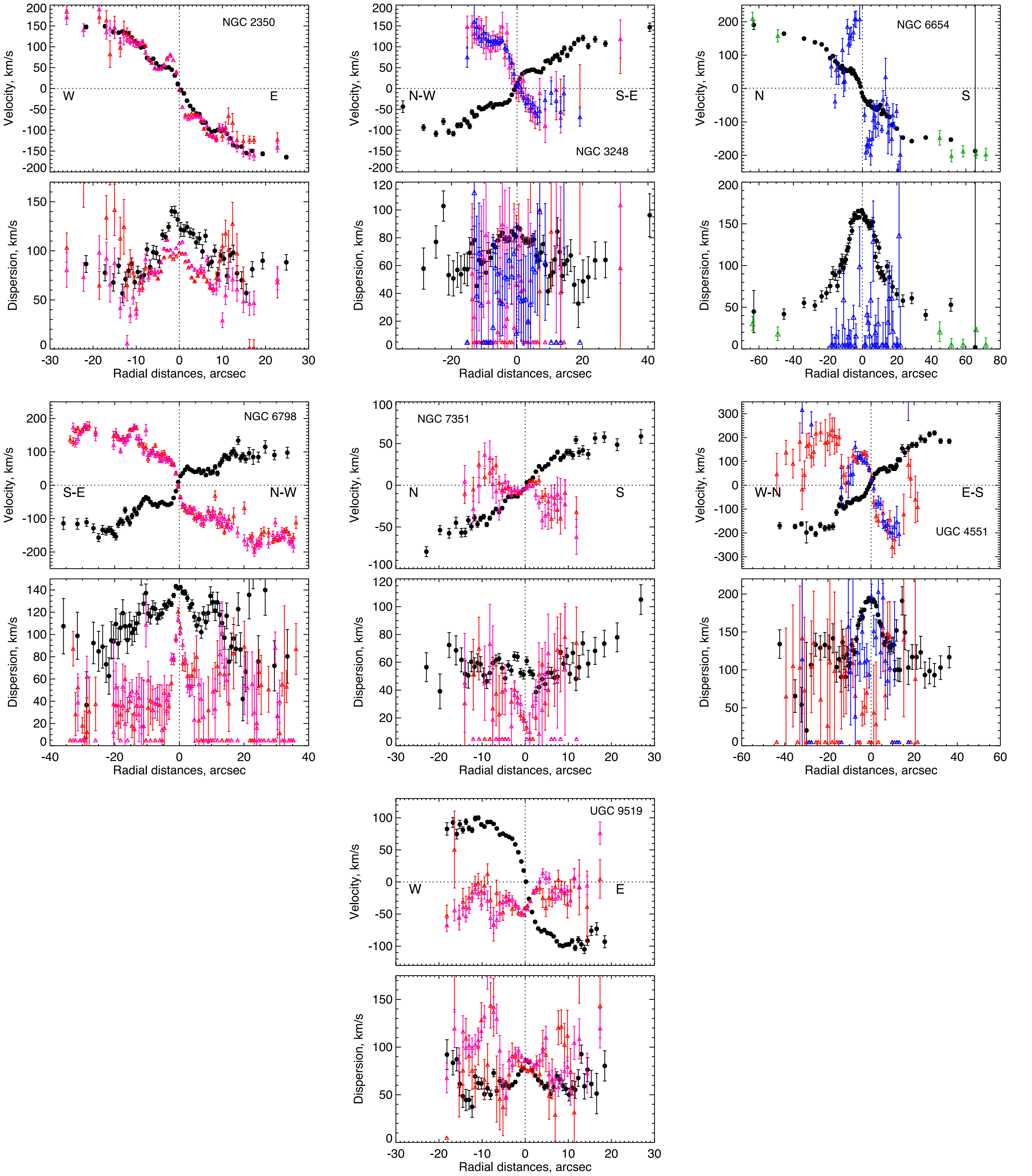

Figure 1. Kinematical profiles of stars (black symbols) and ionized gas (colour symbols) along the major axes. Different colours of symbols correspond to kinematics measured in different emission lines: Hα – red, [N II] – magenta, [O III] – blue, and Hβ – green. The low-velocity dispersions falling below the possibility of being measured with our spectral resolution are indicated as 5 km s^{-1} velocity dispersions.

shown in Fig. 1. In all galaxies, where emission lines were detected, the derived profiles are extended both for the stars and ionized gas.

To identify the dominant source of the gas ionization, we plot our measurements of the emission-line fluxes on to the classical diagnostic BPT diagram (Baldwin, Phillips & Terlevich 1981) (Fig. 2). In order to derive the line ratio estimates for the BPT diagram we needed higher signal-to-noise ratios (S/N) than those required only to constrain kinematics. As a result, we have plotted measurements where the emission lines Hβ, [O III], Hα and [N II] are detected all with S/N>3. Symbol colours code the distance from the centres of the galaxies.

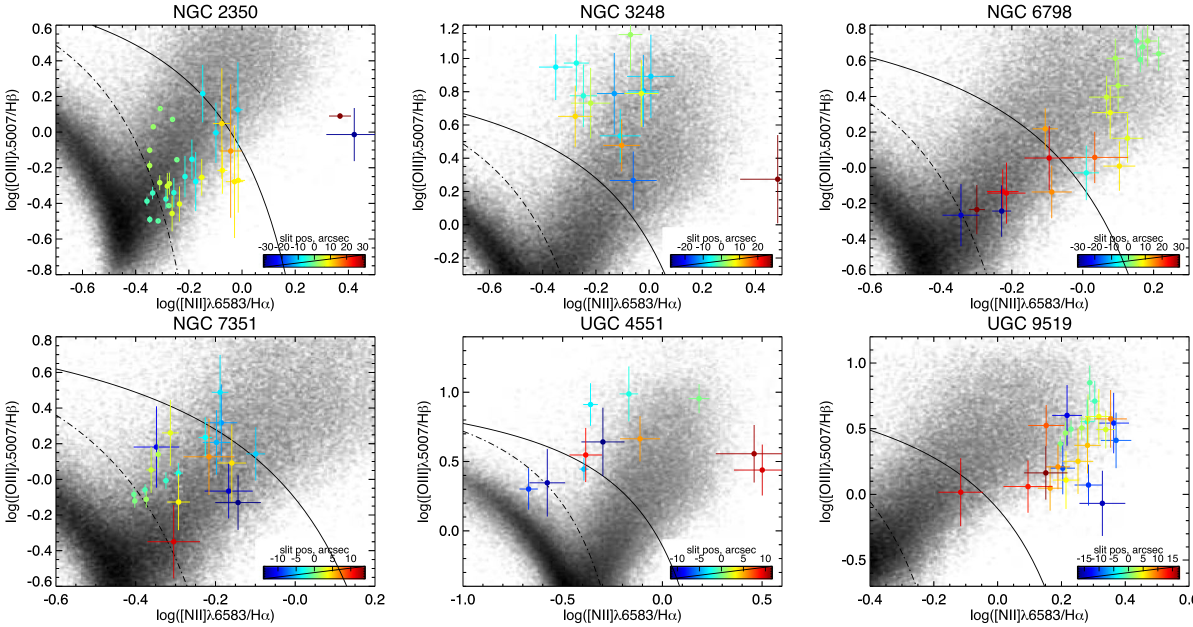

Figure 2. Excitation diagnostic diagrams comparing the emission-line ratios: [N II]/Hα versus [O III]/Hβ. The colour of the points codes the distance from the galaxy centres. The distribution of the measurements of the line ratios for galaxies from the Sloan Digital Sky Survey (SDSS) with high signal-to-noise ratios (S/N > 3 in every line) are shown by grey colour. The black curves, which separate the areas with the AGN/LINER excitations (to the right) from areas with the SF-induced excitation (to the left from these curves), are taken from Kauffmann et al. (2003, dash-dotted curve) and from Kewley et al. (2006, solid curve).

Almost all measurements in NGC 2350 and 7351 as well as in the outer ring of NGC 6798 are located in the BPT diagram region where the SF excitation mechanism dominates. Emission-line measurements for the other galaxies – NGC 3248, UGC 9519 and the greater part of UGC 4551 – fall into the AGN/LINER-dominated (or shock-dominated) region of the BPT diagram.

3 RESULTS: COUNTERROTATION

We found that in our small sample of 12 galaxies observed with the SCORPIO-2, seven (7/12; 58 ± 14 per cent) have revealed extended emission lines. Among those, five galaxies (5/7; 71 ± 17 per cent) demonstrate decoupled gas kinematics with respect to their stellar components over the whole discs. Because we have only long-slit measurements, we characterize the decoupled gas kinematics as 'counterrotation', though in some cases very different amplitudes of the LOS velocity variations for the cold stellar component with negligible asymmetric drift and ionized gas along the major axes (lines of nodes of the stellar discs) indicate different planes of gas and star rotation.

NGC 2350 is characterized by gas emission extending up to 25 arcsec (≈3.5 kpc), and all the gas corotates the main stellar disc. The gas has two peaks at the velocity dispersion profile at radii $r = -17$ arcsec and $r = 12$ arcsec, where the galaxy image reveals bar 'ansae' features.

In NGC 3248, the gas LOS velocity profile has an asymmetric shape: the north-west side has higher velocity amplitude than the south-east side. Probably, this asymmetry is associated with the unsettled state of the gas subsystem. This galaxy is included in the ATLAS-3D sample and is studied with the IFU spectrograph SAURON. The maximum rotational velocity reached within the SAURON field of view, $k_1 = 87.4$ km s^{-1}(Krajnović et al. 2011), is consistent with our long-slit measurements. Davis et al. (2011) detected misalignment between the ionized gas and stars ($\psi_{\rm ion\text{-}star} = 179\overset{\circ}{.}5 \pm 9\overset{\circ}{.}8$) in NGC 3248. Unfortunately, the gas velocity fields are unavailable for most ATLAS-3D galaxies, and we cannot confirm our findings of velocity asymmetries using the IFU data. However, the similar positional angles of the kinematical major axes for the gaseous and stellar velocity fields, though indicating against radial inflows, do not exclude off-plane gaseous motions.

NGC 6654 is an example of weak emission lines. This galaxy was observed using an instrumental set-up covering only Hβ and [O III] lines. The [O III] doublet shows an intense increase of the relative LOS velocity amplitude up to 200–250 km s^{-1}in the central few arcsec being perhaps decoupled though not counterrotating with respect to stars. It then falls to the stellar rotation velocity level at a radial distance of 10–15 arcsec. The kinematics of the Hβ emission line follows the stellar rotation; this line is visible only in a few spatial bins at large radial distances, $R > 40$ arcsec. NGC 6654 was studied as a double-barred candidate by Moiseev (2011) who used the Multi-Pupil Fiber Spectrograph (MPFS) at the 6-m Russian telescope. Moiseev has shown that there is no non-circular motion in the stellar velocity field on the scale of a photometric secondary bar which was then expected in *N*-body simulations. We have reanalysed the MPFS science-ready cube for NGC 6654, which has been kindly provided by Alexey Moiseev, in the same manner as our long-slit data. The stellar velocity field and velocities of the [O III] emission line are presented in Fig. 3. We can see that ionized gas has a similar kinematical major axis as the stars but the velocity amplitudes are quite different and both are consistent with our long-slit measurements. To explain extreme visible velocity amplitudes of the ionized gas, we have considered the possibility of planar non-circular gas motions within the triaxial potential of a nuclear bar with a radius of 4 arcsec which is known in this galaxy (Erwin & Sparke 2002). However, the orientations of both bars in NGC 6654, PA = 13° for the

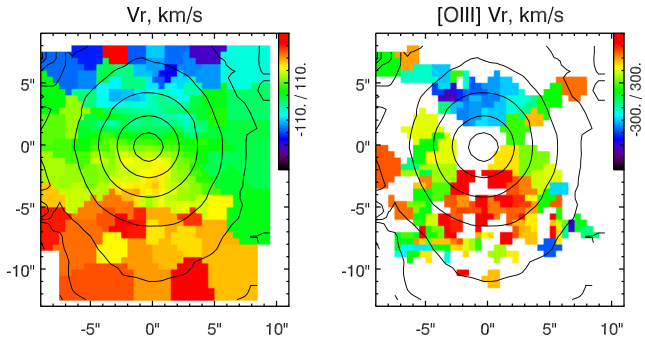

Figure 3. The results of the analysis of the MPFS data cube for NGC 6654. The stellar LOS velocity map is shown in the left-hand panel, while the ionized gas velocity map measured in the [O III] line is shown in the right-hand panel. Note that the amplitudes of velocities are very different.

primary one and PA = 135° for the secondary one (Laurikainen et al. 2011), differ substantially from the disc line of nodes orientation and are not orthogonal to it. Thus, the gas affected by these bars must demonstrate the turn of the kinematical major axis away from the disc line of nodes. Because we do not observe such a turn, we conclude that the only possible explanation of the fast visible gas rotation is that we are looking at the gaseous disc under a larger inclination than at the stellar disc of the galaxy. So, the stellar and gaseous discs are again decoupled.

Another galaxy with a very extended gaseous disc is NGC 6798. However, in this galaxy, the gas counterrotates with respect to the stars. Our measurements reach the radius up to 35 arcsec (5.2 kpc) and reveal a slightly higher amplitude of the gas rotation curve with respect to the stellar one. Such behaviour is expected because of the asymmetric drift taking into account sufficiently high stellar velocity dispersion in the disc of this galaxy. The gas counterrotation continues beyond the optical borders of the galaxy as H I mapping shows (Serra et al. 2012). NGC 6798 also was considered by Davis et al. (2011) who calculated the angle between the kinematical axes of stars and gas $\psi_{\text{ion-star}} = 174\overset{\circ}{.}0 \pm 6\overset{\circ}{.}9$.

NGC 7351, a dwarf S0 galaxy, also has weak emission lines with a relatively large scatter of measurements. Despite this, the gaseous kinematical profile in Fig. 1 clearly indicates the decoupled kinematical properties of the ionized gas in this galaxy beyond the very central part, $R > 5$ arcsec.

The ionized gas kinematics in UGC 4551 has a complex character. Relative LOS velocities of the gas rise rapidly in the central region, then the amplitude falls to null and the north-western side of the velocity profile rises to 200 km s^{-1}with a following decline.

UGC 9519 has emission-line structures extending (projecting?) all over the stellar disc of the galaxy. The low-velocity amplitude of the gas when compared to the stars indicates that the gas rotates in another plane than the stars. The warped polar disc in this system has already been mapped by Serra et al. (2012) in the 21-cm line of the H I. The polar rotation of the molecular and ionized gas rotation is reported by Alatalo et al. (2013) and Davis et al. (2011, 2013). The conclusion about the polar orientation of the gaseous disc in the very centre of the galaxy is also supported by a circumnuclear red dust lane visible in the SDSS images of the galaxy, which is roughly perpendicular to the major axis of the central isophotes (to the bar?). The whole picture is consistent with the gaseous disc, polar in the centre and strongly warped farther from the centre. Let us note that systematic velocities of the gaseous and stellar subsystems differ by 30–40 km s^{-1}, and the symmetry centre of the gas velocity profile is also shifted with respect to the galactic centre along the slit. Perhaps, the gas subsystem of UGC 9519 was accreted recently and has not settled down yet.

4 DISCUSSION AND CONCLUSIONS

We have studied a sample of 12 highly isolated S0 galaxies by means of long-slit spectroscopy undertaken with the reducer SCORPIO-2 of the Russian 6-m telescope. In seven galaxies, we have found extended gaseous discs, and in five galaxies the extended emission-line gas counterrotates their stellar components. The gas excitation is found to be mostly shock-like though a few star-forming rings may be suspected.

By comparing our results on the frequency of extended ionized-gas discs in S0 galaxies with the earlier statistics, we see full agreement. Kuijken, Fisher & Merrifield (1996) found ionized gas in 17 of 29 S0s studied, so their fraction of gas-rich S0s is about 58 ± 9 per cent, just as in our study. However, if we consider a fraction of counterrotating gaseous discs among all extended gaseous discs in S0 galaxies, we see a prominent difference. When S0 galaxies were selected over all types of environment, the fraction of counterrotating gaseous discs was 20–24 per cent (Bertola et al. 1992; Kuijken et al. 1996); more exactly, by combining two samples, Kuijken et al. (1996) gave 24 ± 8 per cent. In our sample, the fraction of counterrotating gaseous discs is 71 ± 17 per cent. We expected such a trend because Davis et al. (2011) noted a dependence of gas kinematics in the early-type galaxies (mostly S0s in the ATLAS-3D sample) on their environment: dense environment provided a tight coincidence between gas and star kinematics while in more sparse environments the fraction of decoupled gaseous kinematics grew. Our isolated S0 galaxies represent an extreme point in this dependency, and the fraction of decoupled gas kinematics exceeds 50 per cent. Following the logic of Bertola et al. (1992), according to which when gas is accreted, it should have an arbitrary spin, long-slit spectroscopy should reveal an equal fraction of corotating and counterrotating gaseous discs. If we take into account the possibility of internal gas incidence, the fraction of systems with counterrotating gaseous discs would be less than 50 per cent. However, our results based on the sample of galaxies in the strictly sparse environment suggest that the fraction of gas counterrotations is higher than 50 per cent. Hence, we can conclude that in isolated S0s their gas is virtually always accreted from external sources. However, to be certain that the directions of possible gas accretion are distributed isotropically, we must first identify sources of gas accretion. Our galaxies are isolated so they cannot acquire their gas from neighbours of comparable mass/luminosity; the sources of cold gas accretion may be dwarf satellites merging (Kaviraj et al. 2009, 2011) or perhaps cosmological gas filaments (Kereš et al. 2005; Dekel & Birnboim 2006). Are they distributed isotropically? This is a good question.

4.1 Dichotomy of gas excitation

It is clear, though not from long-slit data along major axes alone, that generally the gaseous discs in S0s are not coplanar to stellar discs. Thus, what we call ‘counterrotation’ may be the projection of an inclined gaseous disc on to the stellar disc plane. Perhaps there exists a dichotomy concerning the mechanisms of ionized-gas excitation in the discs of S0 galaxies.

Wakamatsu (1993) showed that the shocks can be generated when gas on polar orbits crosses the potential well of a stellar disc, just as the grand-design shock waves in spirals or along the bars of barred galaxies are generated by stellar density enhancements.

In this sense, the inclined gaseous discs are similar to polar ring/disc structures. So, in the cases of gas motions in inclined planes, the shock-like excitation of the gas is expected, and emission-line ratio measurements should be found in the LINER region of the BPT diagram. Another mechanism providing LINER-like emission is ionization by evolved stars during the very hot and energetic post-asymptotic giant branch (post-AGB) phase. It is thought to be especially important in early-type galaxies (Sarzi et al. 2010; Bremer et al. 2013; Singh et al. 2013). Both mechanisms ionize the gas without involving the radiation field of young massive stars. It is expected that both mechanisms would lead to ionization only at the region where gas crosses the galaxy plane due to short cooling time compared to dynamical time. The gradient in excitation should be visible in the IFU data.

When the gas is accreted smoothly in the plane of a stellar disc, there are more possibilities to conserve its coolness with the following ignition of SF. The location of emission-line ratio measurements in the SF region of the BPT diagram supposes that the radiation of young stars contributes the dominant source of gas ionization. Through the observational data presented here, we see that in the galaxies where the gas is probably confined to the disc planes (NGC 2350, 6798, 7351 and the very outer part of NGC 6654) the excitation by young stars is preferable. Shocks or post-AGB stars are the main agent of gas excitation in the remaining galaxies (NGC 3248, UGC 4551, UGC 9519) whose velocity profiles indicate asymmetries and complex features that probably result from the gas motions in the inclined planes.

Earlier, we observed this dichotomy when we found counterrotating gas in S0 galaxies NGC 2551 and 5631 (Sil'chenko, Moiseev & Afanasiev 2009). The coplanar discs of NGC 2551 look UV-bright in the *GALEX* data, so intense SF proceeds over the counterrotating gaseous disc in this galaxy. However, in NGC 5631 the gaseous disc is inclined, and there are no prominent signs of SF in it but the emission-line ratios all over the disc demonstrate the excitation dominated by shocks or old post-AGB stars. Similarly, we have found the shock-like excitation of the emission-line gas in the inclined gaseous disc of S0 galaxy NGC 7743 (Katkov, Moiseev & Sil'chenko 2011). One more example of current SF in the counterrotating gaseous disc coplanar to a main stellar disc represents the lenticular galaxy IC 719 reported by us recently (Katkov, Sil'chenko & Afanasiev 2013). Earlier, this galaxy was observed in the frame of the ATLAS-3D project by Alatalo et al.(2013).

ACKNOWLEDGEMENTS

We thank Alexei Moiseev for providing some observations at the 6-m telescope and the science-ready MPFS cube of NGC 6654. The authors thank the anonymous referee for constructive advice that helped us to improve the paper. The work was supported by the Russian Federation President's grant MD-3288.2012.2 and the Russian Foundation for Basic Research (project nos. 13-02-00059a and 12-02-31452). IYK is grateful to Dmitry Zimin's non-profit Dynasty Foundation.

REFERENCES

Afanasiev V. L., Moiseev A. V., 2011, Bal. Astron., 20, 363
Alatalo K. et al., 2013, MNRAS, 432, 1796
Baldwin J. A., Phillips M. M., Terlevich R., 1981, PASP, 93, 5 (BPT)
Bertola F., Buson L. M., Zeilinger W. W., 1992, ApJ, 401, L79
Bremer M., Scharwächter J., Eckart A., Valencia S. M., Zuther J., Combes F., Garcia-Burillo S., Fischer S., 2013, A&A, 558, A34
Chilingarian I., Prugniel P., Sil'Chenko O., Koleva M., 2007a, in Vazdekis A., Peletier R., eds, Proc. IAU Symp. Vol. 241, Stellar Populations as Building Blocks of Galaxies. Cambridge Univ. Press, Cambridge, p. 175
Chilingarian I. V., Prugniel P., Sil'Chenko O. K., Afanasiev V. L., 2007b, MNRAS, 376, 1033
Davis T. A. et al., 2011, MNRAS, 417, 882
Davis T. A. et al., 2013, MNRAS, 429, 534
Dekel A., Birnboim Y., 2006, MNRAS, 368, 2
Erwin P., Sparke L. S., 2002, AJ, 124, 65
Karachentsev I. D., Makarov D. I., 2008, Astrophys. Bull., 63, 299
Karachentsev I. D., Makarov D. I., Karachentseva V. E., Melnyk O. V., 2011, Astrophys. Bull., 66, 1
Katkov I. Y., Chilingarian I. V., 2011, in Evans I. N., Accomazzi A., Mink D. J., Rots A. H., eds, ASP Conf. Ser. Vol. 442, Astronomical Data Analysis Software and Systems XX. Astron. Soc. Pac., San Francisco, p. 143
Katkov I. Y., Moiseev A. V., Sil'chenko O. K., 2011, ApJ, 740, 83
Katkov I., Sil'chenko O., Afanasiev V., 2013, ApJ, 769, 105
Kauffmann G. et al., 2003, MNRAS, 346, 1055
Kaviraj S., Peirani S., Khochfar S., Silk J., Kay S., 2009, MNRAS, 394, 1713
Kaviraj S., Tan K-M., Ellis R. S., Silk J., 2011, MNRAS, 411, 2148
Kereš D., Katz N., Weinberg D. H., Davé R., 2005, MNRAS, 363, 2
Kewley L. J., Groves B., Kauffmann G., Heckman T., 2006, MNRAS, 372, 961
Krajnović D. et al., 2011, MNRAS, 414, 2923
Kuijken K., Fisher D., Merrifield M. R., 1996, MNRAS, 283, 543
Laurikainen E., Salo H., Buta R., Knapen J. H., 2011, MNRAS, 418, 1452
Le Borgne D., Rocca-Volmerange B., Prugniel P., Lançon A., Fioc M., Soubiran C., 2004, A&A, 425, 881
Makarov D. I., Karachentsev I. D., 2009, Astrophys. Bull., 64, 24
Makarov D., Karachentsev I., 2011, MNRAS, 412, 2498
Moiseev A. V., 2011, Mem. Soc. Astron. Ital. Suppl., 18, 153
Pogge R. W., Eskridge P. B., 1993, AJ, 106, 1405
Sage L. J., Welch G. A., 2006, ApJ, 644, 850
Sarzi M. et al., 2010, MNRAS, 402, 2187
Serra P. et al., 2012, MNRAS, 422, 1835
Sil'chenko O., Moiseev A., Afanasiev V., 2009, ApJ, 694, 1550
Singh R. et al., 2013, A&A, 558, A43
van Dokkum P. G., 2001, PASP, 113, 1420
Wakamatsu K-I., 1993, AJ, 105, 1745
Welch G. A., Sage L. J., 2003, ApJ, 584, 260
Welch G. A., Sage L. J., Young L. M., 2010, ApJ, 725, 100
Young L. M. et al., 2011, MNRAS, 414, 940
Zeilinger W. W., Bertola F., Buson L. M., 1993, in Danziger I. J., Zeilinger W. W., Kjär K., eds, ESO Conf. Workshop Proc. Vol. 45, Structure, Dynamics and Chemical Evolution of Elliptical Galaxies. ESO, Garching, p. 593

This paper has been typeset from a TEX/LATEX file prepared by the author.